Synergistic influence of pH and temperature on rheological behavior of adhesive emulsions stabilized with micelle dispersion of anionic surfactant

Partha Kundu[1†], Vimal Kumar[1*], Peter J Scales[2], Indra Mani Mishra[3]

[1]Department of Chemical Engineering, Indian Institute of Technology Roorkee, Roorkee 247667, Uttarakhand, India

[2]Department of Chemical and Biomolecular Engineering, The University of Melbourne, Parkville,Victoria 3010, Australia

[3]Department of Chemical Engineering, Indian Institute of Technology (Indian School of Mines), Dhanbad, Dhanbad 826004, Jharkhand, India

*Corresponding author: Vimal Kumar (chemdch2015@gmail.com; vksinfch@iitr.ac.in)

Abstract

The influence of emulsion pH and temperature on the rheological behavior of adhesive oil-in-water (o/w) emulsions stabilized with anionic surfactant (SDBS) was studied. The flow properties of emulsions as a complex fluid were investigated using steady and dynamic rheometry for characterization of non-Newtonian behavior. Emulsion pH was varied from 2-12 and temperature was varied from 20-50 ^{o}C respectively. The influences of the above-mentioned variables on the rheology of o/w emulsion were studied using steady shear and dynamic oscillatory experiments. Various viscosity models (2, 3 and 4 parameter rheological model) were used to predict the rheological parameters. An increase in the pH of the emulsion led to an increase in emulsion stability, viscosity and viscoelastic properties (G', G'', η^* and $\tan\delta$), and decrease in the mean droplet size of the emulsion. A decrease in the temperature yields higher values of steady-shear viscosity and viscoelastic properties upon a decrease in droplet size. Emulsions were characterized as flocculated structured liquid exhibiting a characteristic crossover frequency (ω^*) within the range of angular frequency studied in oscillatory

This is the author manuscript accepted for publication and has undergone full peer review but has not been through the copyediting, typesetting, pagination and proofreading process, which may lead to differences between this version and the Version of Record. Please cite this article as doi: 10.1002/jsde.12220

measurements. Overall, emulsions exhibited non-Newtonian shear thinning behavior and synergy of pH and temperature significantly influence the emulsion rheology.

Keywords: Emulsion; Anionic surfactant; Viscoelasticity; Rheology; Non-Newtonian fluids.

Introduction

The rheology of emulsions is a subject of immense importance from both fundamental and applied points of view. Emulsions are encountered in petroleum production (drilling fluids), food industry, pharmaceutics (mainly cosmetics), environmental applications (e.g. aquifer remediation), explosives, paints and polymers [1-4]. The rheology of emulsions is a reflection of the various interactive physico-chemical and electrostatic forces acting in the system [5]. Oil-in-water (o/w) emulsions are usually characterized by a complex rheological behavior due to the collective interactions of surface charge, droplet size distribution, phase volume fraction, continuous-phase ionic strength, dispersed-phase viscosity, and the chemical structure of the emulsifier.

Rheological measurements (steady state, controlled stress and oscillatory measurements) provide information on physical stability and micro-structure of the emulsion. In dynamic (oscillatory) oscillatory measurements, the response of a viscoelastic material (emulsions) subjected to a sinusoidal strain is monitored as a function of the amplitude and frequency of the strain [6]. The phase angle shift (δ) between stress and strain, is given by:

$$\delta = \Delta t \omega \tag{1}$$

where ω is the frequency (rad.s^{-1}) ($\omega = 2\pi\upsilon$, where υ is the frequency (s^{-1})). From the measurement of the angular deflection (using a transducer) and the resulting torque the rheological parameters-the storage modulus (G'), the loss modulus (G''), the complex modulus (G^*) and the complex viscosity (η^*) can be determined. The modulus G' is the measure of the

energy stored elastically in the system, whereas G'' is a measure of the energy dissipated as viscous flow. The viscoelasticity originates from the energy stored at the o/w interface of droplets. The viscoelastic properties of the emulsions depend on the state of flocculation. At moderate to high volume fractions, droplet deformation occurs due to volumetric constraints which causes an increase in surface area and results in energy storage at the interface (elastic energy) [7].

Goodwin et al. [8] experimentally measured the wave rigidity modulus (at a frequency of 1200 rad/s) of weakly flocculated colloidal dispersions (monodisperse polystyrene lattices, at high electrolyte concentrations and with a nonionic surface surfactant). Shear wave propagation measurements were used to quantify the viscoelastic properties of the systems by measurement of the shear wave rigidity modulus. Woutersen and de Kruif [9] related the rheology (steady shear viscosity) of adhesive hard sphere dispersions (SW50/benzene) to the strength of the attractive interaction between the dispersed particles. They performed viscosity measurements of adhesive dispersion as a function of shear rate, volume fraction, and temperature. Woutersen et al. [10] investigated the shear-distorted microstructure of a concentrated dispersion (silica stabilised dispersion) of adhesive hard spheres in the low shear rate regime ($Pe \leq 1$) using a small-angle neutron scattering experiment. They observed that the potential interactions between the particles are controlled by the temperature. At high temperatures the only direct interactions are hard sphere repulsions. Mason et al. [11, 12] experimentally studied bulk elasticity and yield transition of concentrated monodisperse emulsions as a function of volume fraction and droplet size. They observed that the surface elasticity of surfactant significantly influence the emulsion viscosity. Liu et al. [13] discussed about the anomalous viscoelastic behavior of concentrated emulsions and proposed a model predicting the square root of frequency contribution to the complex dynamic shear modulus which was correlated with the experimental observations. Pal [14] reported the effect of droplet size and droplet size distribution on the steady and oscillatory behavior of o/w and w/o emulsions. Trappe and Weitz [15] investigated the scaling behavior of weakly attractive colloidal suspension (colloidal carbon in oil) as a function of particle volume

fraction and interaction potential. They presented a model that accounts for the scaling by combining the elasticity of a solid network formed by the particles and the viscosity of the suspending fluid. Santos et al. [16] investigated the rheology of concentrated o/w emulsions stabilized by mixtures of ethoxylated surfactants and normal alcohols. They observed that the droplet size had a direct impact on emulsion stability and apparent viscosity. The literature survey showed that there are only a few reports on viscoelastic behavior of adhesive (o/w) emulsions. Therefore, it is necessary to study the viscoelastic behavior of such emulsions for fundamental understanding of these complex fluids.

Except for very dilute emulsions, most emulsions exhibit non-Newtonian flow behavior. They also exhibit time-dependent viscoelastic behavior: i.e. they exhibit both viscous and elastic responses under deformation. This requires that the flow data to be interpreted carefully. The objective of the present study was to investigate the influence of pH and thermal stress on the rheological properties of adhesive o/w emulsions using an anionic surfactant. The viscoelastic properties, of ionic o/w emulsions were also discussed in details. The rheological behavior of o/w emulsions are modeled using rigorous non-linear regression analysis of experimental data. The Arrhenius model was used to discuss the effect of temperature on both steady and dynamic (viscoelastic) rheological behavior of o/w emulsions.

Experimental

Chemicals

NaOH (RFCL, New Delhi), anhydrate Na_2SO_4 (Rankem, New Delhi), sodium dodecyl benzene sulfonate (SDBS) (Himedia, Mumbai), NaCl (SRL, Mumbai), Na_2CO_3 (NICE, Cochin) and light Petroleum oil (Indian Oil Corporation Ltd.). The deionized water was used throughout the experiments. All chemicals were used as received.

Preparation of emulsions

Different o/w emulsions were prepared with 30% (v/v) light petroleum oil. The emulsions were prepared by rigorous shearing of the oil and water in a high shear mixer at 30^{o}C. An anionic surfactant (SDBS) was used as a surfactant for the preparation of o/w emulsion. The surfactant concentration was fixed at 1 wt%. The o/w emulsions were prepared by "agent-in-water" method. Details of emulsion preparation can be obtained from elsewhere [17-19]. Surfactant (SDBS) was dissolved in the continuous phase (aqueous phase) and then mixed thoroughly while adding the oil phase slowly. Emulsion pH was adjusted between 2-12 by adding 1(N) HCl and 1(N) NaOH solutions to the continuous phase. After preparation, all emulsions were stored in a thermostatic vessel. Emulsions were characterized by measuring droplet size distribution and zeta potential (Malvern Nano ZS 90, UK).

Rheological Measurements

The rheological properties of emulsions were measured using a controlled-stress rheometer (Physica MCR 100, Anton Paar, Germany) equipped with an EC motor (electronically commutated synchronous motor). These measurements were made under both controlled stress (CS) and controlled strain (CR) modes. A cone and plate geometry was used to make shear stress/shear rate rotation tests. A Peltier cylinder temperature system TEK150P was used for precise temperature control of the lower plate geometry. The temperature of the sample compartment was controlled using a water bath/circulator Viscotherm VT2 Temperature Controller System (TCS) (Anton Paar, Germany). Both steady shear and oscillatory measurements were performed. The steady-shear measurements were carried out over a shear rate range of 10^{-3}–10^{3} s^{-1}. The steady shear viscosity measurements were carefully performed for all emulsion samples. In steady rate sweep measurement equilibrium time was set as 10s for each single data point ensuring viscosity data acquired under steady state conditions. At higher shear rates ($\dot{\gamma} \geq 10^{2}$) time required to reach the equilibrium is less as compared to low shear rates ($\dot{\gamma} \leq 10^{0}$). Thus, for better reproducibility of the viscosity data point 10s was set as an equilibrium time within the shear rate range of 10^{-3}–10^{3} s^{-1}. During steady shear flow experiments, the shear

rate was applied to the emulsion samples as a step function (stepped flow) with step time of 10s and the shear rate was increased logarithmically. The resulting viscosity measurements were performed when the sample reached equilibrium, ensuring the steady shear flow and giving a single viscosity data point at a particular shear rate.

Oscillatory measurements were made to study the viscoelastic behavior of the emulsions. Initially, amplitude sweeps (AS) were performed to establish the linear viscoelastic range of emulsion samples. Then frequency sweeps (FS) were performed within the range of the angular frequency (ω) 1-10^2 s^{-1} to characterize the viscoelastic behavior of the emulsion. Triplicate sample runs were taken. For each steady and oscillatory measurement, fresh sample was used. The plate and cone section of the rheometer was thoroughly cleaned with Millipore water and acetone between each measurement of different emulsion samples.

All rheological measurement was carried out with fresh emulsions immediately after preparation. Emulsion samples were gently and carefully mixed before measurements to avoid phase separation and air entrapment and results were showed as average value (mean percent deviation lower than 10%).

Statistical Analysis

Non-linear regression analysis was carried out for the rheological data and the analysis of variance (ANOVA) at alpha level (sensitivity of regression) of 0.05 was performed to establish the influence of different variables. The best fit to the model was selected on the basis of correlation coefficient (R^2) and χ^2.

Results and Discussions

Physicochemical Properties of Adhesive O/W Emulsions

Emulsions were found to be stable and flocculated in nature. The degree of flocculation was found to increase as the pH of the emulsion decreases. The details physicochemical

characteristics of emulsions were shown in Table 1. It was observed that the mean droplet diameter of emulsions was decreased with increase in emulsion pH. Due to the fact that with an increase in pH favoring droplet–droplet collision and preventing coalescence. It was observed that as temperature increases mean droplet diameter of emulsions also increases due to the coalescence of emulsion droplets.

The magnitude of the zeta potential and electrophoretic mobility of o/w emulsions increases with increase in pH. This indicated that the electrostatic repulsion among the charged droplets progressively increased with an increase in pH.

Rheological behavior under steady shear flow

Fig.1 shows that the emulsions exhibit shear-thinning behavior, with a clear tendency of both a zero-shear rate-limiting viscosity (η_0), at low shear rates and a high-shear rate-limiting viscosity (η_∞), at high shear rates. This kind of flow behavior is observed in flocculated emulsions due to the droplet-droplet deflocculation mechanism [20]. A hump was observed at low shear rate ($\dot{\gamma} \sim 10^{-3}$ s^{-1}) for pH 12 and pH 10. At a shear rate of 0.002 s^{-1}, a yield point was observed and thereafter, shear-thinning behavior was observed. The shear-thinning behavior was manifest because of the gradual break-up of inter-particle fluid structure (flocculated droplets) [21]. Furthermore, hydrocluster groups of particles/ droplets whose relative motions are restricted by lubrication stresses are responsible for shear thickening. Shear thinning arises from the decreased relative contribution of entropic forces among the dispersed droplets [22]. For pH12 and pH10, the dilatant behavior was observed at $\dot{\gamma} < 0.002$ s^{-1}.This shear rate of $\dot{\gamma}_c = 0.002$ s^{-1} may be seen as the critical shear rate below which no structural deformation occurred due to very low applied shear stress against the strong flocculation force. The yield point gets diminished with decrease in pH (pH< 10), and no hump was observed in the low shear rate region. From Table 1, it was observed that d_m shifted toward larger droplet size as the pH of the emulsion decreases. Thus, the droplet size of the emulsion was large as compared to that for pH 12 and 10. Therefore, the

structural deformation of the emulsions occurred continuously from flocculated to a deflocculated state under applied shear rate even at lower values overcoming the weak flocculation force.

Fig. 1 shows that the o/w emulsions at different pH exhibit non-Newtonian flow behavior within the measured range of shear rate (10^{-3} - 10^{3} s^{-1}). However, the continuous phase (water and 1 wt% surfactant) also exhibited non-Newtonian shear-thinning behavior. The emulsion flow spectra showed three distinct flow regimes, i.e. low shear rate, intermediate and high shear rate regime. Various non-Newtonian rheological models: (Ostwald-de Waele, Cross, Carreau, and Sisko) were evaluated to satisfactorily represent the non-Newtonian behavior of the o/w emulsions.

Ostwald-de Waele (Power law) model: $$\eta_a = K\dot{\gamma}^{n-1} \quad (2)$$

Sisko model: $$\eta_a = \eta_\infty + K\dot{\gamma}^{n-1} \quad (3)$$

Cross model: $$\frac{\eta_a - \eta_\infty}{\eta_0 - \eta_\infty} = \left[1 + \left(\frac{\gamma}{\gamma_c}\right)^m\right]^{-1} \quad (4)$$

Carreau model: $$\frac{\eta_a - \eta_\infty}{\eta_0 - \eta_\infty} = \left[1 + \left(\frac{\gamma}{\gamma_c}\right)^2\right]^{-N} \quad (5)$$

Rheograms for emulsions at pH 12 and pH 10 showed complex behavior. Fig. 1 clearly shows that the power law model cannot represent the shear stress-shear rate data over the entire range of shear rate. At low shear rate region ($\dot{\gamma} < 0.1$ s^{-1}), the power law model did not fit well. However, the power law model was satisfactory for the intermediate shear rate region $\left(10^{-1} s \le \dot{\gamma} \le 10^{3} s^{-1}\right)$, for all the sets of o/w emulsions $\left(2 \le pH \le 12\right)$. The regression analyses are shown in Table S1. It is observed that the average flow behavior index (n) for all o/w emulsions lies between 0.55 and 0.89, which exhibits the shear-thinning pseudoplastic nature of the emulsion. These may be due

to the droplet aggregation and the structural breakdown of the emulsions due to the hydrodynamic force generated during shearing. It was also observed that the flow behavior index (n) decreases, with an increase in pH of the emulsions. Thus, the pseudoplasticity of o/w emulsions increases with an increase in pH and becomes more shear thinning in nature. The flow consistency index (K) of emulsions also increases with an increase in pH.

Both the Cross model (Eq. 4) and Carreau model (Eq. 5) take into account the two limiting viscosities, zero shear viscosity, η_0 and infinite shear viscosity, η_∞ over the entire range of shear rate studied. Best fitted Carreau model for all rheological data points of emulsions was shown in Fig. 1. The characteristic parameters of the Cross and Carreau models from their fit to experimental data are shown in Table 2. The experimental rheological data well describe by both this model with the average R^2 value of 0.99 for $(2 \le pH \le 8)$. But the rheological behavior of the emulsions at pH 10, and pH 12 was difficult to model due to high non-linearity in the rheogram. For pH 10 and pH 12, two shear thinning regimes were observed: one at low shear rate zone (3×10^{-3} - 4×10^{-2} s^{-1}), and the other at a relatively higher shear rate zone (10^0-10^3 s^{-1}). In between these two zones, a plateau region was observed, which decreases at lower pH.

It was observed from the Fig. 1, that for pH of 8 and below the curves reach a zero-shear plateau with a steadily increasing zero-shear viscosity. However a departure of this for pH 10 and 12 with a sudden jump to a larger value was observed. This is an indication of a liquid-solid (sol-gel transition) due to electrostatic repulsions which enhances the stability of the emulsion and may even form a weak crystalline solid [23]. These shear induced phenomena also termed as Shear banding (SB) which observed in variety of other complex fluids, such as lamellar surfactant phases [24, 25], wormlike micelles [26, 27], suspensions [28] and polymeric solutions [29, 30]. SB phenomena is the stratification of the flow into regions of high and low shear rate, $\dot{\gamma}$, connected by an "interface" of sharp $\dot{\gamma}$ change in which this homogeneous velocity gradient profile becomes unstable to heterogeneous perturbations and splits into high and low shear rate bands that coexist in the cell, so that the local shear rate varies spatially $\dot{\gamma} = \dot{\gamma}(y)$. Thus, a characteristic stress plateau was observed in the flow curve at low shear rate regime. It occurs in

homogeneously sheared systems when there is a range of shear rates where the stress apparently decreases with increasing shear rate, before it resumes its ascent. The molecular origin of this double-valuedness in the constitutive behavior is usually the existence of at least two separate relaxation mechanisms, each being prevalent at a disparate region of the $\dot{\gamma}$ spectrum [31].

Scaling (Master curve) the rheological response of adhesive (o/w) emulsions

Master curve was constructed by superposition method using a dimensionless viscosity and shear rate by using an empirically calculated shift factor. Values of the shift factors for the different emulsions studied, as a function of pH, are shown in Fig. 2. A dimensionless viscosity, including both the zero-shear rate and the high-shear rate-limiting viscosities was obtained from the fitting of the Carreau model. Thus, $\eta'_{red} \equiv \alpha_{pH}.\eta_{red}$ vs. $\dot{\gamma}$ leads to an empirical master curve that describes the flow behavior of these emulsions in the entire range of pH studied, where α_{pH} was the empirical shift factor (Fig. 2), which is equal to 1 for the reference flow curve (pH = 12) and $\eta_{red} = (\eta - \eta_\infty)/(\eta_0 - \eta_\infty)$. However, pH dependence of shift factor must provide information about the influence of pH on viscous behavior of emulsion. This parameter gives information about the resistance of the emulsion microstructure to a shear induced breakdown process in the shear-thinning region.

Rheological behavior under dynamic oscillatory shear flow

The viscoelastic behavior of o/w emulsions were assessed by dynamic oscillatory measurement in terms of dynamic moduli G' and G'' as a function of frequency. G' is a measure of the energy stored and recovered per cycle of deformation reflecting the elastic part of the emulsion. The loss modulus is a measure of the energy lost per cycle and reflects the liquid-like component of the emulsions.

The linear viscoelastic region of o/w emulsions was established by an amplitude sweep (AS) test. Thereafter, the frequency sweep (FS) tests were performed for all emulsions at a

constant stress (0.5 Pa) in the linear viscoelastic region. The evolution of the storage modulus (G'), loss modulus (G''), complex viscosity (η^*) and loss tangent (tan δ) with frequency (ω) for all emulsions at different pH are shown in Fig. 3. From this figure, it was observed that G' and G'' increases with an increase in frequency. Both G' and G'' were functionally dependent on frequency, which indicated that the o/w emulsions are flocculating in nature. It was observed that in the lower frequency regime ($\omega \leq 40$ s^{-1}), G'' is greater than G' and attains a certain characteristic frequency (ω^*), which was referred to as the cross-over frequency. At the cross-over frequency (ω^*), G' equals G''. Above this frequency, G'' decreases and G' becomes greater than G''. This kind of behavior was observed for the emulsion system [6]. This also shows that the emulsion behaves more like an elastic fluid. The dynamic response of the continuous phase reveal that aqueous 1 wt% surfactant (SDBS) solution was viscous as the loss modulus (G'') falls above the storage modulus (G') over the range of frequency (Fig. S1).

The pH played a prominent role in the changing the flow behavior of the emulsions. With a decrease in the pH, the emulsion stability decreases with the consequent decreases in G', and the emulsion behaves more like a viscous fluid than an elastic fluid. The emulsion was more stable at pH 12 than that at pH 2. The presence of repulsive force among the charged droplets at the water (high dielectric fluid) and oil (low dielectric fluid) interface helps stabilize the emulsion. This arises because of an asymmetric distribution of counter-ions at the interface, creating a dipole normal to the fluid/fluid interface [32]. This prevents the droplet-droplet coalescence. As the pH increases, zeta potential of the emulsion increases enhancing the repulsive force at the interface (Table 1). At a higher pH (pH 12), the surfactant produces a thin viscoelastic film at the o/w interface. This hinders coalescence of droplets, and the emulsion droplets behave like hard spheres. As a consequence, the emulsion showed elastic behavior [33]. As the pH decreases, the charges at the interface get gradually neutralized and the surfactant separates out from the o/w interface, causing film drainage and a gradual decrease in emulsion stability. Thus, the emulsion shows an increasing viscous behavior with a decrease in the pH of

the emulsion. From Fig. 3, it was observed that G' decreases with a decrease in the emulsion pH. The gap between G' and G'' also increases with a gradual shift in ω^* to the higher side of frequency.

Modeling the dynamic viscoelastic behavior of adhesive o/w emulsions

The dynamic rheological data (frequency versus G' and G'') of different emulsions were described by a power-law type model as shown below:

$$G' = K'(\omega)^{n'} \qquad (6)$$

$$G'' = K''(\omega)^{n''} \qquad (7)$$

where K', K'', n' and n'' were estimated from the rigorous non-linear regression of Eq. 6-7. The model parameters are shown in Table 3. The loss modulus showed a shear-thinning behavior (n'' < 1) due to shear induced structural breakdown of the viscous emulsions. Mechanical spectra of the elastic moduli show highly non-linear behavior and exhibit shear-thickening behavior (n' >1) due to the macro-molecular aggregation. It was found that G' was a strong function of frequency, and the (G'-G'') crossover frequency leads to the inference that the emulsion behaves like a weak gel [34].

The mechanical spectra of the dynamic moduli (Fig. 3), shows the variation of G' and G'' with frequency. In the experimental frequency range, a plateau region was observed. This may be ascribed to the extensive flocculation of the surfactant molecules at the o/w interface under shear [35]. In the plateau region tan δ passes through a minimum which is characterized by the plateau modulus (G_P^0).The plateau modulus is a viscoelastic parameter which was obtained by the extrapolation of the entanglement contribution to G' at higher frequencies. G_P^0 was estimated using the following relation:

$$G_P^0 = [G']_{\tan\delta \to minimum} \quad (8)$$

The cross over frequency is also characterized by the cross over moduli (G_C) which was defined as:

$$G_C = [G_{\bar{\omega}}]_{G' = G''} \quad (9)$$

The variation in the value of G_P^0 and G_C with the pH of the emulsion is shown in Fig.4. It was found that both these moduli increase logarithmically with an increase in the emulsion pH as the viscoelasticity of the emulsion increases.

The steady-state apparent viscosity at zero shear ($\eta_{a,0}$) is less reliable than the value at the low shear ($\dot{\gamma} = 0.01 s^{-1}$). The low-shear apparent viscosity was given as:

$$\eta_{a(001)} = |\eta_a|_{\dot{\gamma}=0.01} \quad (10)$$

The evolution of low-shear steady-state viscosity, $\eta_{a(0.01)}$ with emulsion pH is shown in Fig. 4. The low-shear apparent viscosity, $\eta_{a(0.01)}$ increases logarithmically with an increase in the emulsion pH. A similar tendency was found for linear viscoelasticity functions, G_P^0 and G_C of these emulsions. From the droplet size evolution (Table 1), it was observed that the mean droplet diameter decreases with an increase in the emulsion pH. This explains the increase in viscous and viscoelastic functions. The droplet size distribution (DSD) is an important structural parameter which influences the emulsion Rheology significantly [20, 5]. Specially, in the structured macromolecule-stabilized systems (at higher pH), in which inter-droplet interactions may play a key role.

Time-dependent flow behavior of adhesive (o/w) emulsions

The time dependency and the structure recovery of o/w emulsions is shown in Fig. 5. The time-dependency of o/w emulsions was tested in three intervals under controlled shear rate (CSR). The performed tests were simulated using the following shear conditions: rest (pre-shear)-high shearing (structure decomposition)-rest (structure regeneration/recovery).

In the first interval, a constant but low shear rate (1 s^{-1}) was applied to the emulsion for 50 s. In the second interval, a constant but high shear rate (100 s^{-1}) was imposed for 50 s on the emulsion which caused the internal structural decomposition of the emulsions. Thereafter, the imposed high shear rate was withdrawn and the emulsions were allowed to recover their structure under constant low shear rate ($1s^{-1}$) for a long period of time of about 300 s. During the whole shearing period, the resulting change of emulsion apparent viscosity was observed with time as shown in Fig. 5. It was observed that the emulsions exhibit viscoelastic behavior confirming the earlier observations. The effect of emulsion pH in changing the viscoelastic nature of emulsions is significant. The $\eta_a - t$ curve (Fig. 5) shows that the emulsion with different pH exhibited thixotropic behavior. Emulsions of pH 12 and pH 10 exhibited very good regeneration of the complete structure which decomposed during the high shearing process. As the pH decreases, the structure regeneration tendency of the emulsions also decreases. This indicates that the viscoelasticity of the emulsions decreases with a decrease in pH. For the emulsion of pH 8 and pH 6, the decomposed structure regenerates very slowly. For the emulsions having pH 4 and pH 2, the viscosity data showed a wide scatter over the regeneration period. For these emulsions, a transient or unsteady state behavior was observed during the regeneration period. Thus, it can be inferred that the emulsions with pH 4 and pH 2 exhibit poor structure recovery and were not able to regenerate their internal structure over a prolonged regeneration period.

Effect of temperature on steady and dynamic (viscoelastic) rheological behavior of adhesive (o/w) emulsions

The effect of temperature on the rheological behavior of the emulsions (pH = 12, 30% v/v o/w emulsion) is shown in Fig. 6. It was found that the o/w emulsion exhibited temperature-dependent viscous behavior. The apparent viscosity of the emulsions decreases with an increase in temperature. It was observed that the viscous behavior becomes highly non-linear at lower shear rates. The emulsions exhibited the characteristics of non-Newtonian, shear-thinning (pseudoplastic) fluids over the studied temperature range (20-50^{o}C). Various non-Newtonian viscosity models were fitted with the experimental data (Table 2 and Table S2).The non-Newtonian behavior increases strongly with a decrease in temperature. From the power low model, it was observed that the flow behavior index, $n < 1$, and that it decreases with an increase in temperature. This shows inferred that the shear thinning behavior of o/w emulsion increases with a decrease in temperature as also the pseudoplasticity of the emulsions. Evolution of droplet size of o/w emulsions at different temperatures was shown in Table 1. It was observed that as the temperature increases, the DSD curve shifts towards the higher droplet size range with an increase in average droplet size. As the in-situ temperature of the o/w emulsion increases, the disruption of emulsion droplets gets enhanced, and facilitating the droplet coalescence process. This results in the evolution of comparatively larger droplets with a wider DSD spectrum.

From the rheogram (Fig. 6), it was observed that the o/w emulsion exhibited two limiting viscosities over the range of study: the zero shear viscosity (η_0) at low shear rate and the infinite shear viscosity (η_∞) at high shear rate. It was very difficult to model the overall rheological behavior of the emulsions over a wide range of shear rate. In addition to power law model, the rheological data were also fitted to four different viscosity models. The model fitted parameters were shown in Tables 2 and S2. The Carreau model represents the rheological behavior of the o/w emulsion very well over the entire range of shear rate as compared to Cross and Sisko models, with high R^2 value and low error.

The effect of temperature on viscoelastic properties (G', G'' and η^*) of the emulsions in the whole range of applied frequency is shown in Fig. 7. From the mechanical spectra of o/w

emulsions at different temperatures, it was found that the viscoelastic parameters are temperature dependent. G', G'' and η^* decrease with an increase in temperature. It was also found that $G'' > G'$ at lower frequency (below $\omega \sim 30\, s^{-1}$) and $G' > G''$ at higher frequency range (above $\omega \sim 50\, s^{-1}$) with a characteristic crossover frequency (ω_c). The mechanical spectra shows a viscous response of the emulsion at lower frequency and an elastic response at a higher frequency. As the temperature of the emulsion increases, the ω_c shift towards the higher frequency and the emulsion shows viscous behavior at higher frequency. A power-law type model (Eq. 12-13) described well the variation of viscoelastic parameters with temperature (Table 3). All the o/w emulsions at different temperatures were characterized as a weak gel like viscoelastic fluid as the slope (n' and n'') of G' and G'' spectra were positive [36]. The viscoelasticity of the emulsion decreases with an increase in temperature as both K' (0.390-0.0354 Pa.s^n) and K'' (8.364-4.032 Pa.s^n) decrease with an increase in temperature (20-50^{o}C). Furthermore, the exponent of G' and G'' were varied as n' =1.132-1.149 and n'' =0.214-0.203, (Table 4). From these results, it was inferred that the o/w emulsion behaves like a structured liquid over the studied temperature range (20-50 ^{o}C) [37]. The temperature dependency of η_a and η^* is described by an Arrhenius-type relationship, as given below:

$$\eta_a = A exp\left(\frac{-E_\eta}{RT}\right) \tag{11}$$

$$\eta^* = A^* exp\left(\frac{-E_{\eta^*}}{RT}\right) \tag{12}$$

Steady state and dynamic rheological data for $\dot{\gamma} = 10\, s^{-1}$ were fitted to Eqs. (11-12) and the best-fit model parameters were shown in Table 4. It was observed that the complex viscosity (η^*) was always greater than the steady state shear viscosity (η_a) over the temperature range (20-50^{o}C). Both η_a and η^* decrease with an increase in temperature from 20 to 50 ^{o}C due to an increase in the intermolecular distances for thermal expansion. The magnitude of viscous activation energy, $E_\eta > E_{\eta^*}$ implies that the steady-state shear viscosity of o/w emulsion samples were more sensitive to temperature than the complex viscosity. Therefore, the viscosity of emulsions decreases with an increase in temperature accompanied by an increase in mean droplet diameter.

Conclusions

The rheological behavior of adhesive (o/w) emulsions was studied by steady shear and dynamic oscillatory rheology within the linear domain of viscoelasticity. The steady shear test were conducted over a shear rate range of 10^{-3}– 10^3 s^{-1} and the dynamic oscillatory measurements over a frequency range of 1–10^2 s^{-1}. The rheological behavior was investigated by varying the pH (2-12) and temperature (20-50^{o}C). The results indicated that the o/w emulsions stabilized with anionic surfactant behave as non-Newtonian fluids, with shear thinning pseudoplastic characteristic and also exhibited thixotropic behavior.

The viscoelastic properties (G', G'', η^* and $\tan\delta$) were found to be a strong function of angular frequency and exhibited a characteristic cross over frequency (ω_c).For $\omega < \omega_c$, the viscous response is predominating ($G'' > G'$) and for $\omega > \omega_c$, the elastic response ($G' > G''$) was predominating. Thus o/w emulsion can be characterized as a flocculated structured liquid or weak gel. The steady shear rheological behavior of the o/w emulsions exhibited highly non-linear nature, posing difficulty in modeling the experimental data. The four parameter Cross and Carreau model described the emulsion behavior reasonably well over the entire shear rate range (10^{-3}– 10^3 s^{-1}) as compared to other two models (Ostwald-de Waele and Sisko model). The

emulsion rheology was found to be affected significantly by pH and temperature. The viscoelastic properties were also influenced by the pH and temperature. The shear thinning property and the pseudoplasticity of the emulsions decreased with a decrease in pH and an increase in temperature with a corresponding larger average droplet size and a wider DSD. The dynamic moduli (G' and G'') decreases with an increase in temperature and a decrease in pH. The effect of temperature on the steady shear viscosity and viscoelastic properties were investigated by using an Arrhenius type model. It was found that the steady shear viscosity of o/w emulsions was more sensitive to temperature than the complex viscosity $\left(E_{\eta} > E_{\eta^*}\right)$.

Acknowledgements

Authors gratefully acknowledges the financial support by Indian Institute of Chemical Engineers (IIChE), India, (research project-grant IIC-734-CHD) and Science & Engineering Research Board (SERB), Department of Science & Technology, Government of India (R&D project grant SER-924-CHD)for the present work.

References

1. Pal R. (1994) Metering of two-phase liquid–liquid emulsions: a state of the art review. Ind Eng Chem Res 33: 1413–1435.
2. Mirvakili A, Rahimpour M R, Jahanmiri A (2012) Effect of a Cationic Surfactant as a Chemical Destabilization of Crude Oil Based Emulsions and Asphaltene Stabilized. J Chem Eng Data 57: 1689−1699.
3. Kundu P, Mishra, I M (2013) Removal of Emulsified Oil from Oily wastewater (oil-in-water emulsion) using Packed Bed of Polymeric Resin Beads. Sep Purif Technol 118: 519-529.
4. Kundu P, Mishra, I M (2018) Treatment and reclamation of hydrocarbon-bearing oily wastewater as a hazardous pollutant by different processes and technologies: a state-of-the-art review. Rev Chem Eng DOI: https://doi.org/10.1515/revce-2017-0025.
5. Kundu P, Kumar V, Mishra I M (2018) Study the electro-viscous effect on stability and rheological behavior of surfactant-stabilized emulsions. J Dispers Sci Technol 39 (3): 384-394.
6. Tadros T F (1994) Fundamental principles of emulsion applications. Colloid Surf A 91: 39-55.
7. Lacasse MD, Grest GS, Levine D, Mason TG, Weitz DA (1996) Model for the elasticity of compressed emulsions. Phys Rev Lett 76: 3448-3451.
8. Goodwin JW, Hughes RW, Partridge SJ, Zukoski CF (1986) The elasticity of weakly flocculated suspensions. J Chem Phys 85: 559-566.
9. Woutersen ATJM, de Kruif CG. (1991) The rheology of adhesive hard sphere dispersions. J Chem Phys 94: 5739-5750.
10. Woutersen ATJM, Mellema J, Blom C, de Kruif CGJ. (1994) Linear viscoelasticity in dispersions of adhesive hard spheres. J Chem Phys 101: 542-553.
11. Mason TG, Bibette J, Weitz DA (1995) Elasticity of Compressed Emulsions. Phys Rev Lett 75 (10): 2051-2054.

12. Mason TG, Bibette J, Weitz DA (1996) Yielding and Flow of Monodisperse Emulsions. J Colloid Interface Sci 179: 439–448.
13. Liu AJ, Ramaswamy S, Mason TG, Gang H, Weitz DA (1996) Anomalous Viscous Loss in Emulsions. Phys Rev Lett 76 (16): 3017-3020.
14. Pal R (1997) Viscosity and storage/loss moduli for mixtures of fine and coarse emulsions. Chem Eng J 44: 37–44.
15. Trappe V, Weitz DA (2000) Scaling of the Viscoelasticity of Weakly Attractive Particles. Phys Rev Lett 85: 449 –452.
16. Santos RG, Bannwart AC, Loh W (2014) Phase segregation, shear thinning and rheological behavior of crude oil–in–water emulsions. Chem Eng Res Des 92 (9): 1629–1636.
17. Kundu P, Kumar V, Mishra IM (2015) Modeling the steady-shear rheological behavior of dilute to highly concentrated oil-in-water (o/w) emulsions: Effect of temperature, oil volume fraction and anionic surfactant concentration. J Petrol Sci Eng 129: 189-204.
18. Kundu P, Agrawal A, Mateen H, Mishra IM (2013) Stability of oil-in-water macro-emulsion with anionic surfactant: Effect of electrolytes and temperature. Chem Eng Sci 102: 176-185.
19. Kundu P, Paul V, Kumar V, Mishra IM (2015) Formulation development, modeling and optimization of emulsification process using evolving RSM coupled hybrid ANN-GA framework. Chem Eng Res Des 104: 773-790.
20. Otsubo Y, Prudhomme RK (1994) Rheology of Oil-in-Water Emulsions. Rheol Acta 33: 29–37.
21. Lee HM, Lee JW, Park OO (1997) Rheology and Dynamics of Water-in-Oil Emulsions under Steady and Dynamic Shear Flow. J Colloid Inter Sci 185: 297–305.

22. Cheng X, McCoy JH, Israelachvili JN, Cohen I (2011) Imaging the Microscopic Structure of Shear Thinning and Thickening Colloidal Suspensions. Science 333: 1276-1279.
23. Mewis J, Wagner NJ (2012) Colloidal Suspension Rheology, Cambridge University Press.
24. Fan Y, Tang H, Wang Y (2017) Synergistic Behavior and Microstructure Transition in Mixture of Zwitterionic Surfactant, Anionic Surfactant, and Salts in Sorbitol/H_2O Solvent: 1. Effect of Surfactant Compositions. J Surfactants Deterg 20(2): 435–443.
25. Salmon, J. B., Manneville, S., Colin, A., 2003. Shear banding in a lyotropic lamellar phase. I. Time-averaged velocity profiles. Phys. Rev. E. 68 05150, 1-10.
26. Wei Y, Han Y, Zhou H, Wang H, Mei Y (2016) Rheological Investigation of Wormlike Micelles Based on Gemini Surfactant in EG–Water Solution. J Surfactants Deterg 19(5): 925–932.
27. Mei Y, Han Y, Wang H, Xie L, Zhou H (2014) Electrostatic Effect on Synergism of Wormlike Micelles and Hydrophobically Modified Polyacrylic Acid. J Surfactants Deterg 17(2) 323–330.
28. Ragouilliaux A, Herzhaft B, Bertrand F, Coussot P (2006) Flow instability and shear localization in a drilling mud. Rheol Acta 46: 261–271.
29. Ravindranath S, Wang SQ, Olechnowicz M Quirk RP (2008) Banding in simple steady shear of entangled polymer solutions. Macromolecules 41(7): 2663–2670.
30. Kamal M S, Sultan A S, Al-Mubaiyedh UA, Hussien IA, Pabon M (2014) Evaluation of Rheological and Thermal Properties of a New Fluorocarbon Surfactant–Polymer System for EOR Applications in High-Temperature and High-Salinity Oil Reservoirs. J Surfactants Deterg 17(5): 985–993.
31. Tsenoglou C, Voyiatzis E (2008) Steady shear banding in complex fluids. J Non-Newtonian Fluid Mech 151 (1–3): 119–128.

32. Aveyard R, Clint JH, Nees D, Paunov VN (2000) Compression and structure of monolayers of charged latex particles at air/water and octane/water interfaces. Langmuir 16: 1969–1979.

33. Saiki Y, Horn RG, Prestidge CA (2008) Droplet structure instability in concentrated emulsions. J Colloid Inter Sci 320: 569–574.

34. Gunasekaran S, Mehmet AM (2000) Dynamic oscillatory shear testing of foods selected applications. Trends Food Sci Technol 11: 115-127.

35. Jiang LC, Basri M, Omar D, Rahman MBA, Salleh AB, Rahman RNZRA (2011) Self-assembly behaviour of alkylpolyglucosides (APG) in mixed surfactant-stabilized emulsions system. J Mol Liq 158 (3): 175–181.

36. Ross-Murphy SB, McEvoy H (1986) Fundamentals of hydrogels and gelation. Br Polym J 18: 2–7.

37. Sanchez C, Renard D, Robert P, Schmitt C, Lefebvre J (2002) Structure and rheological properties of acacia gum dispersions. J Food Hydrocolloid 16: 257-267.

List of Figures

Fig. 1. Apparent viscosity-shear rate plot of adhesive (o/w) emulsions for different pH.
pH: 12 –■–; 10 –●–; 8 –▲–; 6 –▼–; 4 –◆–; 2 –⬟–.

Fig. 2. pH-Reduced master flow curve with evolution of the shift factor for 30% (v/v adhesive (o/w) emulsions with 1 wt% surfactant concentration.
pH: 12 –■–; 10 –●–; 8 –▲–; 6 –▼–; 4 –◆–; 2 –⬟–.

Fig. 3. Mechanical spectra of o/w emulsions at different adhesive (o/w) emulsion pH.
G'' –□–; G' –■–; η* –●–.

Fig. 4. Influence of pH on the steady-state viscosity at 0.01 s^{-1}, the plateau modulus (G_P^0) and with cross over moduli (G_C) of adhesive (o/w) emulsion. $\eta_{a(0.01)}$ ■; G_P^0 ♦; G_C ◊.

Fig. 5. Time dependent behavior ($\eta_a - t$ plot) of adhesive (o/w) emulsions at different pH.

Fig.6. Rheogram of adhesive (o/w) emulsions at different temperature.

20 °C –■–; 30 °C –●–; 40 °C –▲–; 50 °C –▼–.

Fig. 7. Influence of temperature on the dynamic oscillatory mechanical spectra of adhesive (o/w) emulsions. (a) G' versus ω plot ; (b) G'' versus ω plot ; (c) η^* versus ω plot.

20 °C –■–; 30 °C –●–; 40 °C –▲–; 50 °C –▼–.

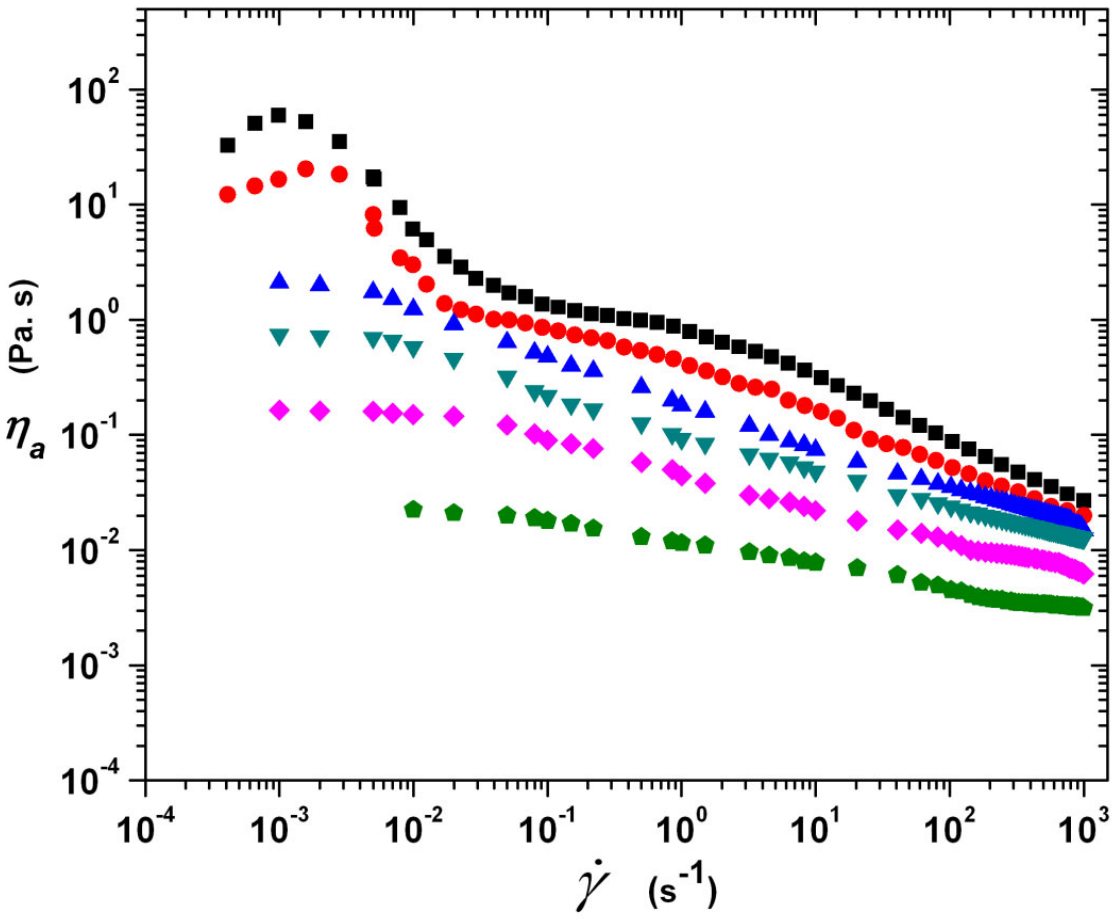

Fig. 1.

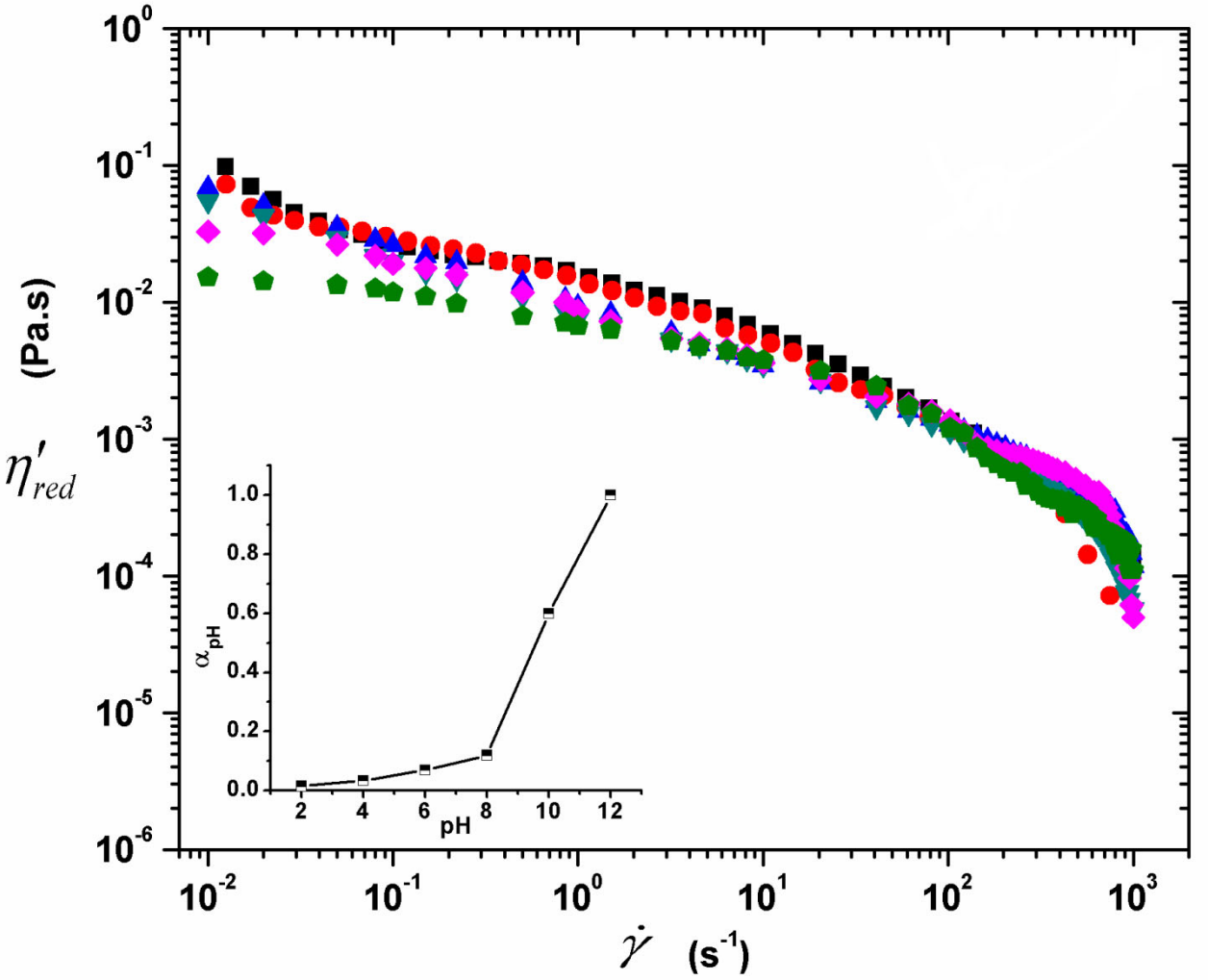

Fig. 2.

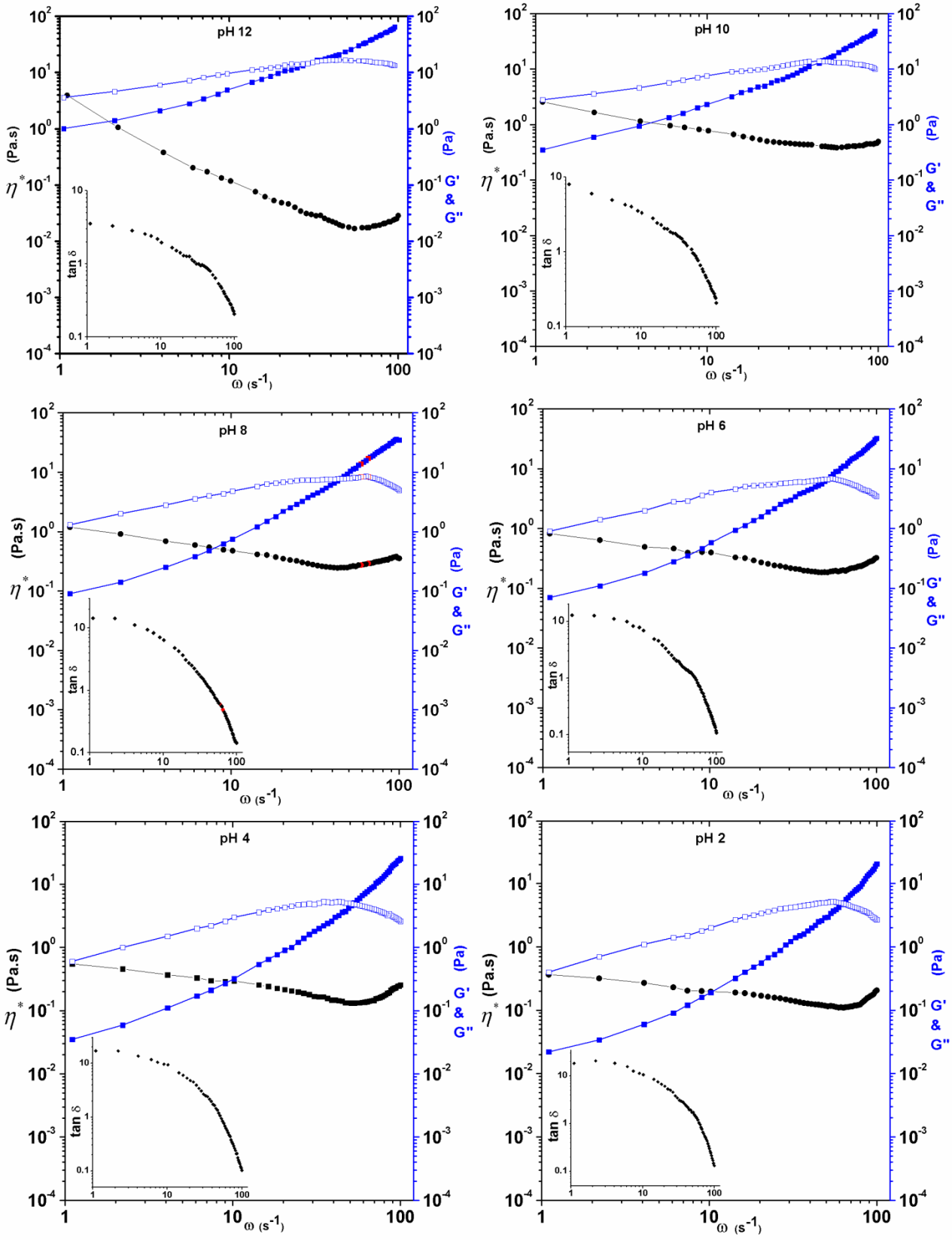

Fig. 3.

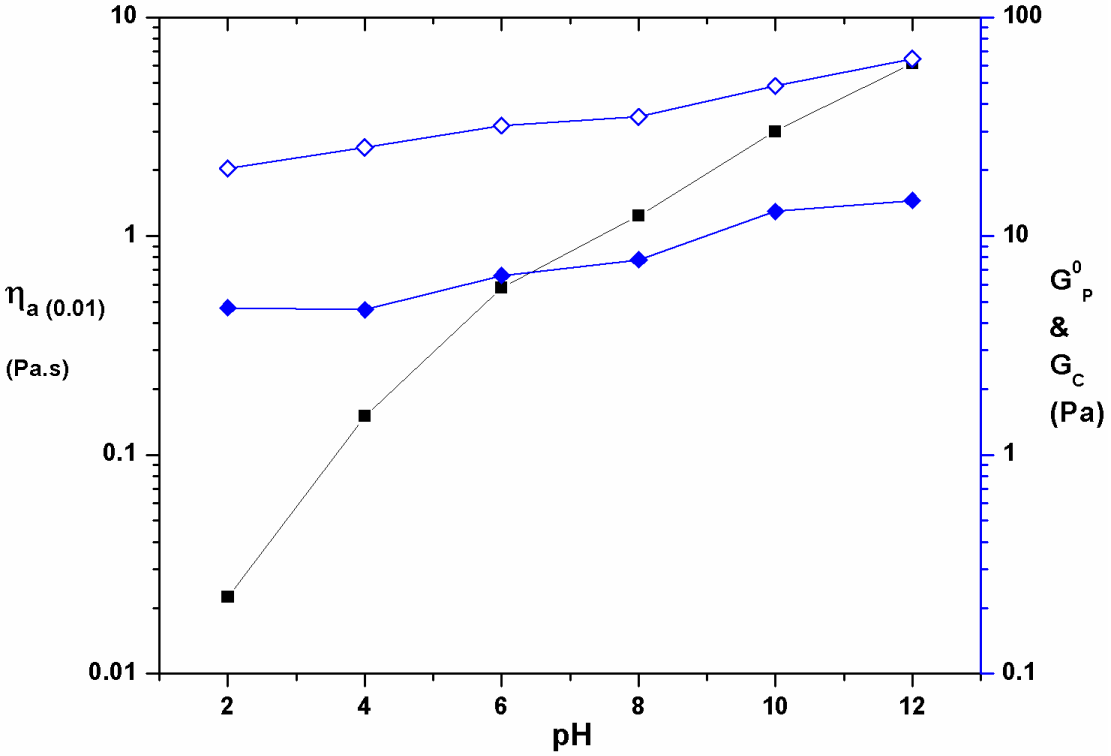

Fig. 4.

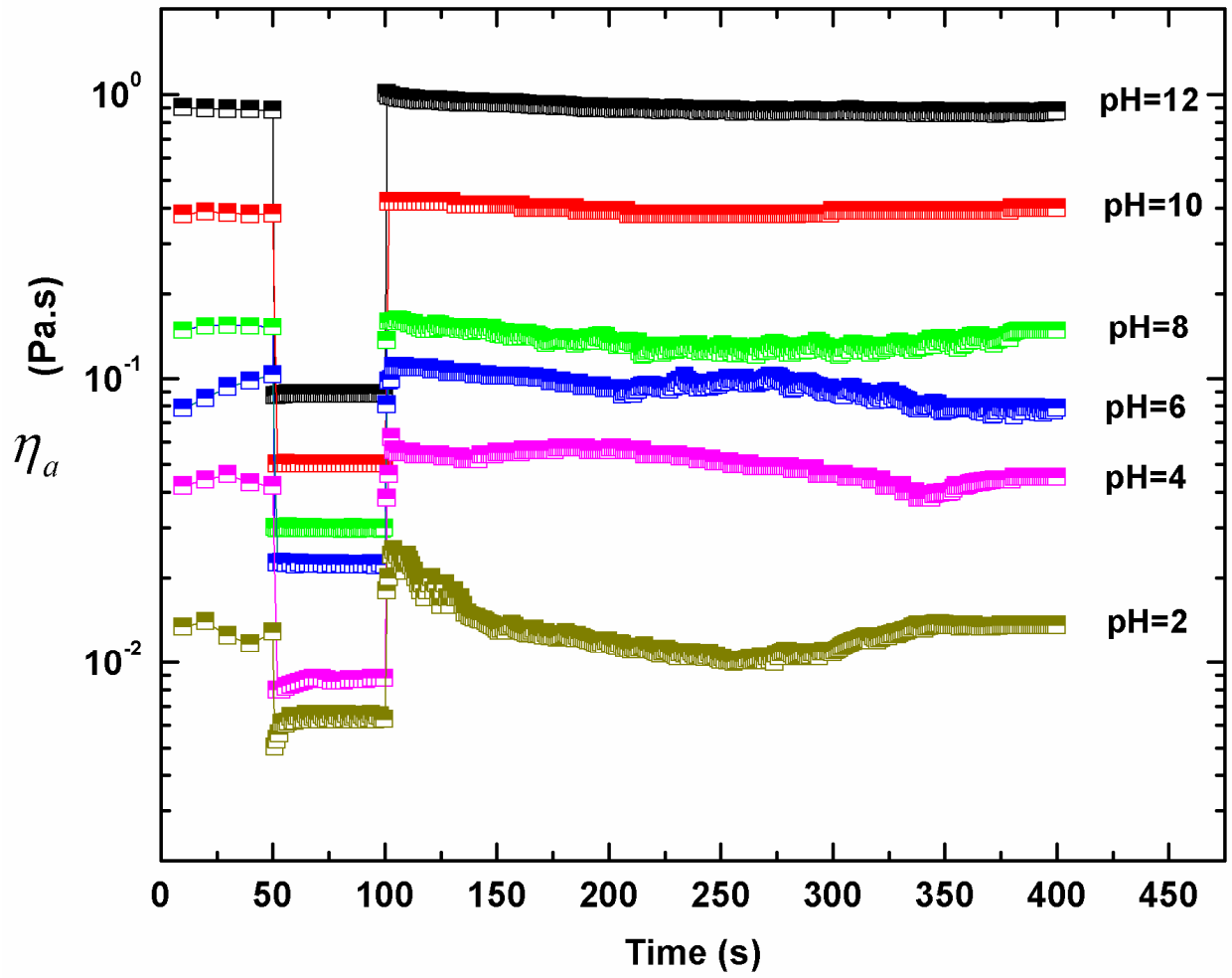

Fig. 5.

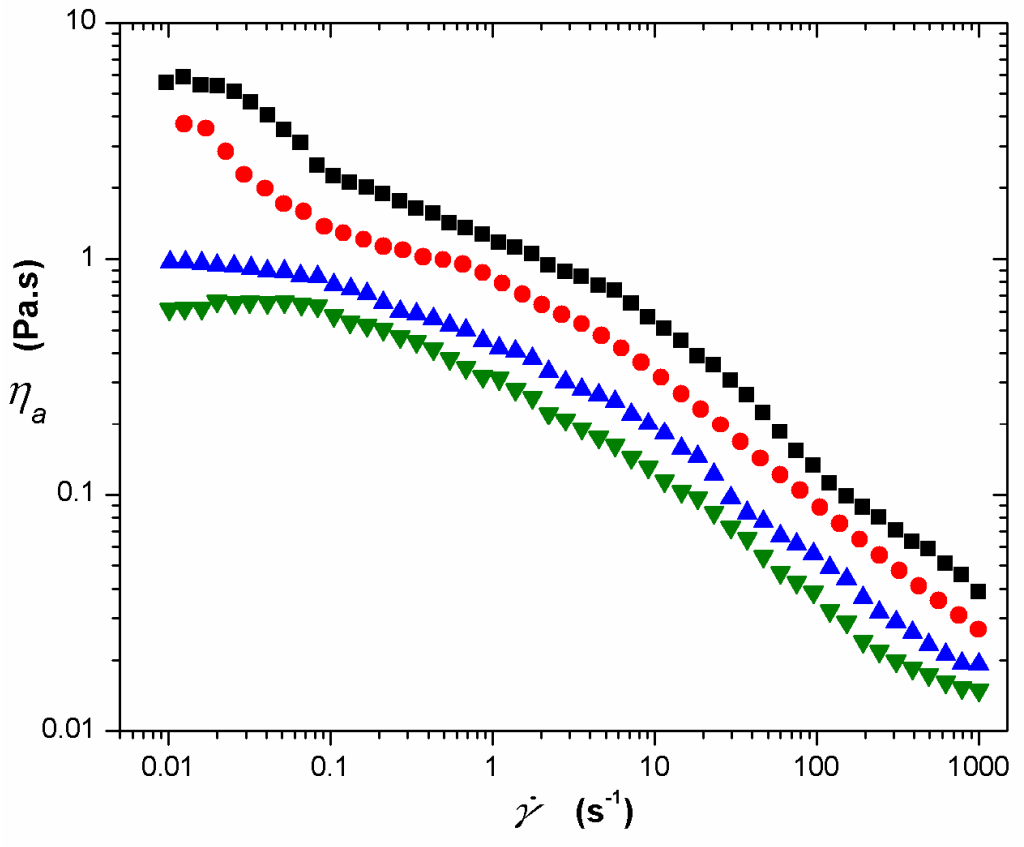

Fig. 6.

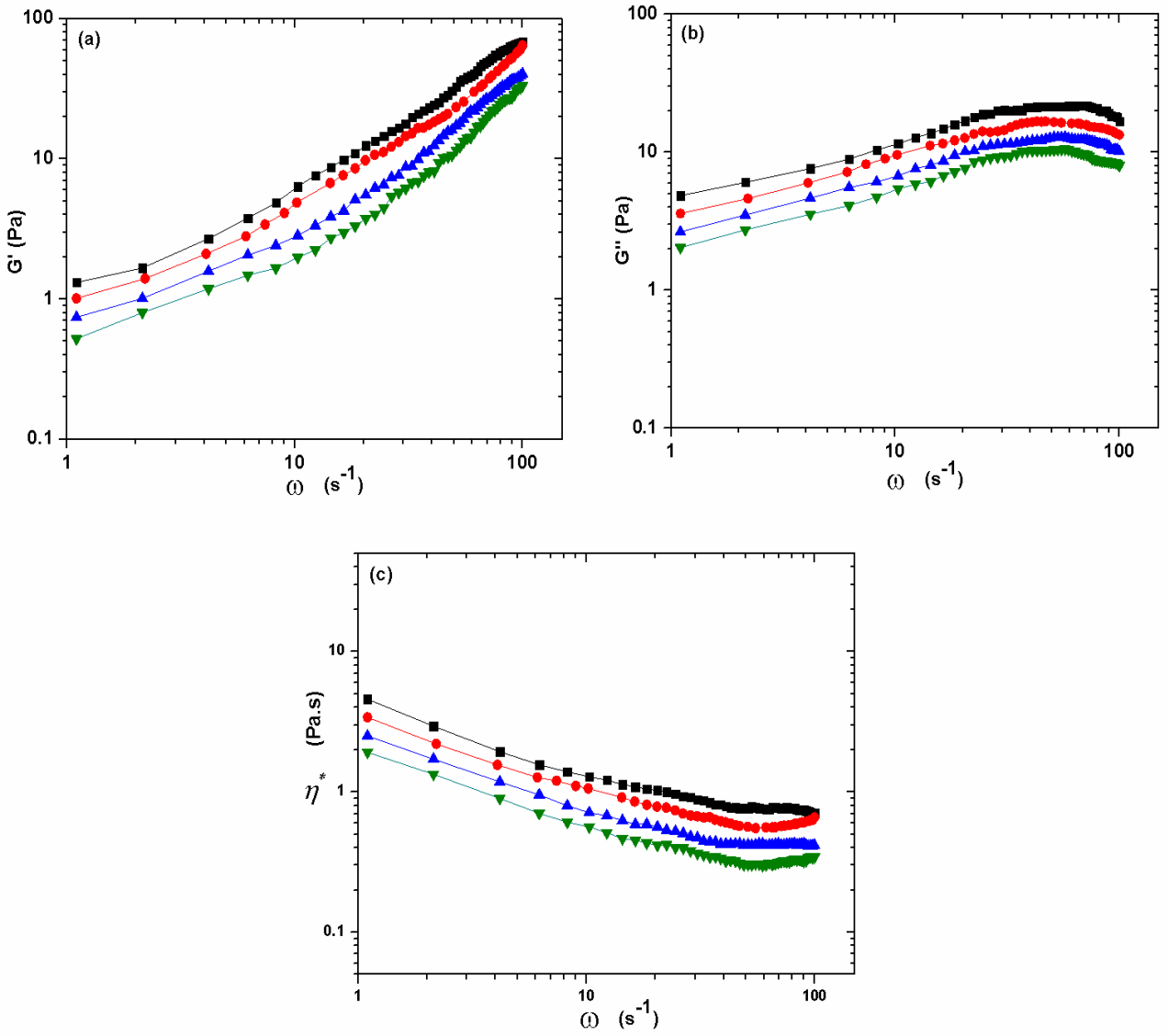

Fig. 7.

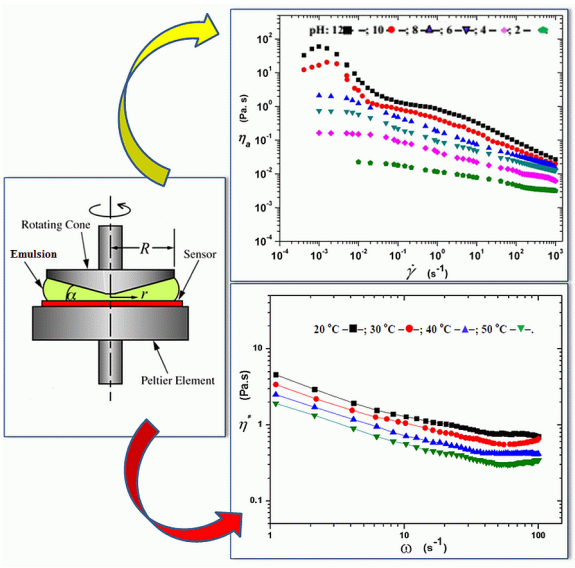

jsd-17-0274-File003.tif

List of Tables

Table 1 : Physicochemical characteristic of adhesive(o/w)emulsions

	Mean droplet diameter (d_m) µm	**Zeta potential (mV)**	**Electrophoretic mobility ($m^2. V^{-1}.s^{-1}$)×10^8**
Emulsion pH			
2	5.73	-33.4	-2.42
4	5.52	-40.4	-3.42
6	1.96	-50.7	-4.02
8	1.82	-57.2	-4.49
10	1.77	-60.4	-5.08
12	1.26	-65.1	-5.62
Temperature (^oC)			
20	1.53	-	-
30	4.00	-	-
40	19.35	-	-
50	21.33	-	-

Table 2. Flow parameters of adhesive (o/w) emulsions determined by Cross and Carreau model.

Cross model						
pH	η_0**(Pa. s)**	η_∞**(Pa. s)**	$\dot{\gamma}_c$ **(s $^{-1}$)**	***m***	χ^2	R^2
12	49.39 ± 1.90	0.832 ± 0.51	0.004 ± 0.0003	2.93± 0.53	10.6	0.949
10	16.52 ± 0.57	0.497 ± 0.18	0.005± 0.0002	4.90± 1.45	1.37	0.946
8	2.75± 0.098	0.024 ± 0.004	0.008 ± 0.001	0.632± 0.023	9.02×10^{-4}	0.996
6	0.841± 0.022	0.019 ± 0.002	0.027± 0.003	0.738± 0.033	2.10×10^{-4}	0.994
4	0.179± 0.003	0.007± 0.0006	0.125± 0.01	0.598± 0.022	7.58×10^{-6}	0.997
2	0.029 ± 0.001	0.002± 0.0002	0.236± 0.058	0.358 ± 0.019	7.03×10^{-8}	0.997
Temperature (^{o}C)						
20	5.88 ± 0.01	0.039 ± 0.01	0.109 ± 0.01	0.774 ± 0.053	0.145	0.952
30	3.73 ± 0.011	0.027 ± 0.01	0.078 ± 0.010	0.627 ± 0.055	0.072	0.920
40	1.094 ± 0.019	0.019 ± 0.01	0.471 ± 0.033	0.580 ± 0.013	2.462×10^{-04}	0.998
50	0.699 ± 0.013	0.015 ± 0.01	0.771 ± 0.066	0.708 ± 0.029	4.014×10^{-04}	0.993
Carreau model						
pH	η_0**(Pa. s)**	η_∞**(Pa. s)**	$\dot{\gamma}_c$ **(s $^{-1}$)**	***N***	χ^2	R^2
12	50.66± 2.04	0.734± 0.55	0.006± 0.003	1.77± 1.14	11.78	0.946
10	16.83 ±0.72	0.409±0.21	0.015 ±0.022	6.30±16.49	1.81	0.933
8	2.15±0.014	0.013±0.002	0.003 ±0.0001	0.227 ±0.003	2.0×10^{-4}	0.999
6	0.746±0.004	0.012±0.001	0.007 ±0.0003	0.228±0.004	3.81×10^{-5}	0.999
4	0.160±0.0008	0.003±0.0005	0.022±0.001	0.171±0.004	2.41×10^{-6}	0.999

2	0.022±0.0002	0.003±0.0003	0.036± 0.003	0.093±0.003	5.49×10^{-8}	0.998
Temperature (^{o}C)						
20	6.528 ± 0.312	0.088 ± 0.061	0.014 ± 0.003	0.220± 0.0145	0.0367	0.988
30	3.730 ±0.01	0.027 ± 0.010	0.012 ± 0.002	0.198 ± 0.0120	0.0338	0.962
40	0.971 ±0.001	0.019 ± 0.001	0.080 ± 0.006	0.181 ± 0.0060	9.191×10^{-04}	0.992
50	0.662 ±0.001	0.015 ± 0.001	0.136 ± 0.009	0.210 ± 0.0069	3.577×10^{-04}	0.994

Table 3. Dynamic shear parameters of power-law functions describing storage and loss moduli of adhesive (o/w) emulsions at different pH and temperature.

pH	$G' = K'(\omega)^{n'}$				$G'' = K''(\omega)^{n''}$			
	K' (Pa.s^n)	n'	χ^2	R^2	K'' (Pa.s^n)	n''	χ^2	R^2
pH12	0.150±0.018	1.30±0.03	2.494	0.993	6.446±0.70	0.209±0.03	3.837	0.692
pH 10	0.028±0.003	1.61±0.03	0.741	0.996	5.043±0.61	0.216±0.03	2.972	0.662
pH 8	0.006±0.0007	1.89±0.03	0.391	0.997	3.645±0.50	0.163±0.04	1.703	0.408
pH 6	0.001±0.0002	2.22±0.03	0.317	0.996	3.069±0.51	0.138±0.04	1.546	0.259
pH 4	0.0002 ±0.0001	2.57±0.04	0.174	0.997	2.514±0.44	0.117±0.05	1.101	0.208
pH 2	$2.95\times 10^{-5} \pm 7.5\times 10^{-6}$	2.91±0.06	0.198	0.994	1.664±0.32	0.219±0.05	0.893	0.422
Temperature (^{o}C)								
20	0.390±0.03	1.132±0.016	1.782	0.996	8.364±0.87	0.214±0.03	6.155	0.691
30	0.150±0.02	1.303±0.027	2.494	0.993	6.446±0.70	0.209±0.03	3.837	0.692
40	0.115±0.007	1.277±0.015	0.416	0.997	4.985±0.51	0.206±0.03	2.046	0.679
50	0.035±0.003	1.486±0.020	0.369	0.996	4.032±0.49	0.203±0.03	1.844	0.597

Table 4. Arrhenius model temperature dependency parameters of adhesive (o/w) emulsions.

Temperature (^oC)	$\eta_a = A\exp\left(\frac{-E_\eta}{RT}\right)$				$\eta^* = A^*\exp\left(\frac{-E_{\eta^*}}{RT}\right)$			
	η (Pa.s)	A (Pa.s^n)	E_η (kJ/mol)	R^2	η^* (Pa.s)	A*(Pa.s^n)	E_{η^*} (kJ/mol)	R^2
20	0.57				1.28			
30	0.32	7.435×10^{-08} ±0.41	38.554	0.998	1.06	1.27×10^{-04} ±0.92	22.543	0.968
40	0.20				0.71			
50	0.13				0.562			